Proceedings of the 17th World Congress
The International Federation of Automatic Control
Seoul, Korea, July 6-11, 2008

Frequency Locking of an Optical Cavity using LQG Integral Control ⋆

S. Z. Sayed Hassen * **E. H. Huntington** * **I. R. Petersen** *
M. R. James **

* *University of New South Wales at the Australian Defence Force Academy, Canberra, ACT 2600, Australia (e-mail:s.sayedhassen, e.huntington, i.petersen@adfa.edu.au)*
** *Australian National University, Canberra, ACT 2600, Australia (e-mail:Matthew.James@anu.edu.au)*

Abstract: This paper considers the application of LQG integral control theory to a problem of cavity locking in quantum optics. The cavity locking problem involves controlling the error between the laser frequency and the cavity frequency. A model for the cavity system, which comprises of a piezo-electric actuator and an optical cavity is determined in the frequency domain using a subspace identification method. An LQG controller which includes integral action is synthesized to stabilize the frequency of the cavity at the laser frequency and to reject low frequency noise inherent in laser systems. The controller is discretized and is successfully tested in the laboratory after being implemented on a dSpace DSP board.

1. INTRODUCTION

Experimental quantum optics is an area in which feedback control is applied to systems whose dynamics are most naturally described using a quantum mechanical description rather than a classical description. Such quantum optical systems have applications in areas such as quantum computing, quantum teleportation, quantum communications, and gravity wave detection.

Fig. 1 shows a photograph of a typical quantum optics laboratory. Quantum optical systems are comprised of optical components (such as mirrors, beamsplitters, optically active materials, etc) and optical subsystems (such as cavities, interferometers, lasers, etc) constructed from these components. Two such subsystems, a cavity and a laser, are indicated.

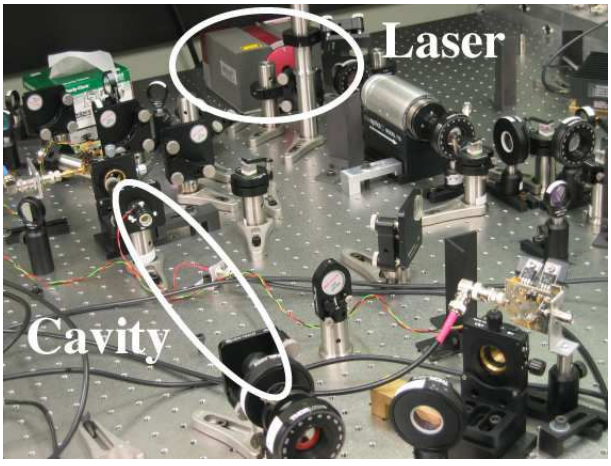

Fig. 1. Photograph of a quantum optics laboratory including cavity system.

⋆ This work is supported by the Australian Research Council.

In this paper, we consider the application of systematic methods of LQG optimal control to a problem of cavity locking which occurs in the area of experimental quantum optics. In this problem, an optical cavity is driven by a laser and a piezoelectric actuator is used to adjust the position of one of the cavity mirrors. This allows the resonant frequency of the cavity to be locked onto the frequency of the laser via the use of feedback control. The most common method which has been used to date to achieve this frequency locking is known as the Pound Drever Hall method; e.g., see Black [2001]. This approach involves measuring the frequency error, commonly referred to as "detuning" variable Δ. In our case, the available measurement y is one of the cavity quadratures which is measured using the standard homodyne detection method; e.g., see Bachor and Ralph [2004]. In addition, we also create a fictitious output from our measured output, which is the integral of the output y. These two outputs are then used to obtain a Kalman state estimate, which when combined with a state feedback optimal control law, allows us to control the slowly varying unmodeled disturbances (low frequency laser noise) present in our system. The cavity locking requirement, which now includes rejecting this disturbance, is reflected in an LQG integral cost functional.

The model of the system is determined by first stabilizing the system. In particular, the data for the plant is gathered when the system is in a closed-loop with a proportional-integral controller in place. In our case, we measure frequency domain data of the plant over a suitable frequency range using a swept sine digital signal analyser. We then use a subspace identification method to determine a linear model in state-space form from the measured data; see McKelvey et al. [1996]. This allows the plant to be modeled as a linear system with reference to a given operating point, where laser locking occurs. Our LQG integral controller design is based on this linear model. The

controller thus obtained is discretized and implemented on a dSpace DSP system in the laboratory. Experimental results were obtained showing that our controller has been effective in locking the optical cavity to the laser frequency.

2. THE CAVITY LOCKING PROBLEM

We begin by considering a model for our cavity system. This cavity system is made up of two parts:

- A mechanical subsystem representing the dynamics of the piezo-actuator, the controlled mirror and the power amplifier driving the actuator;
- An optical subsystem representing the dynamics of the optical cavity (formally this system is a quantum system but in the LQG control problem under consideration, the system can be controlled by controlling an equivalent classical subsystem; e.g., see Edwards and Belavkin [2005]; Shaiju et al. [2007]).

We assume that the laser driving the cavity is in a coherent state (see Bachor and Ralph [2004] for details) since our homodyne detection system uses the laser driving the cavity as the reference oscillator in the homodyne detector. This has the effect of canceling out any common-mode quadrature amplitude and phase variations in the laser and thus our assumption is justified.

The components in the frequency stabilization problem are depicted in Fig. 2. The problem is to regulate to zero the "detuning" Δ between the laser frequency and the natural cavity frequency. This is achieved by controlling the piezo-electric actuator which in turn accurately controls the position of one of the cavity mirrors.

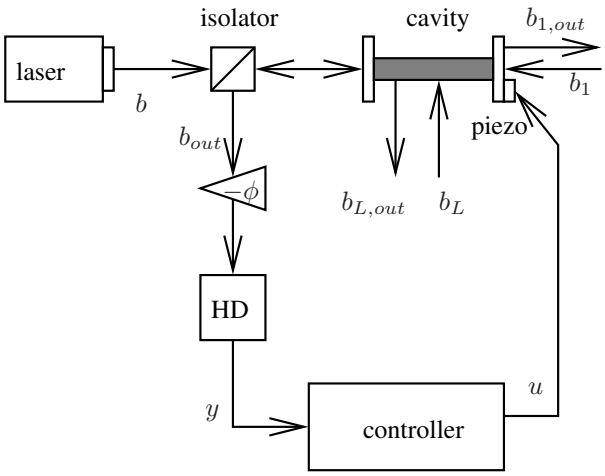

Fig. 2. Cavity locking feedback control loop.

The state of a quantum mechanical system is represented by a vector in a separable Hilbert space. The state ψ is denoted using Dirac's notation as $|\psi\rangle$ in quantum mechanics and is called a *ket*. The laser mode b of frequency ω_0 is represented by a coherent state $|\beta\rangle$, where β is a real number (without loss of generality), modeled by a boson field $b = b_0 + \beta$, where b_0 is a vacuum field, a standard quantum Gaussian white noise (with unit variance), Gardiner and Zoller [2000]. In addition to the source laser mode b, the cavity is also coupled to two other optical fields: a transmitted mode b_1, and a loss mode b_L (these respective input fields are both standard vacua).

A quadrature of the laser field reflected by the cavity b_{out} is continuously measured by homodyne detection, producing a classical electrical signal y. This signal is processed by a classical computer producing an electrical control signal u, which influences the position of the cavity mirror via a high voltage amplifier and a piezo-electric actuator.

3. MODELLING AND SYSTEM IDENTIFICATION

Our cavity system, referred to as the cavity in Fig. 2 can be further subdivided as shown in Fig. 3. It comprises of an electro-mechanical subsystem (piezo-electric actuator and high voltage amplifier) and the optical cavity. In practice, the control signal u together with a noise process w_1 feeds into the mechanical subsystem generating Δ at its output. The "detuning" Δ represents the frequency deviation of the cavity's resonant frequency from the laser frequency ω_0. However, Δ is not available for measurement and instead we have the signal y which is the output of the optical cavity. The signal y is measured using a standard homodyne detection method and also includes the sensor noise w_2. In addition, there are other noise sources that enter the optical cavity which are referred to generally as quantum noises here and these are discussed in more detail in Sec. 3.2.

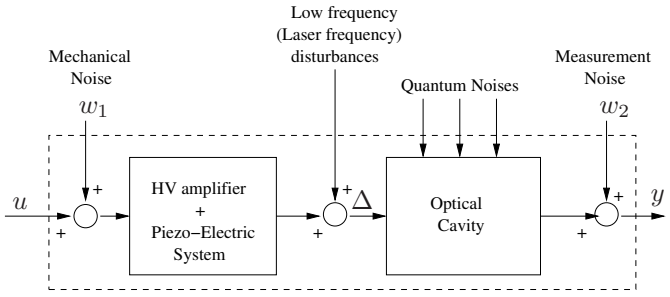

Fig. 3. Block diagram of the cavity system.

3.1 The Optical Cavity

The cavity is described by the following set of equations:

$$\begin{aligned} \dot{a} &= -(\frac{\kappa}{2} + i\Delta)a - \sqrt{\kappa_0}(\beta + b_0) \\ &\quad -\sqrt{\kappa_1}b_1 - \sqrt{\kappa_L}b_L \\ b_{out} &= \sqrt{\kappa_0}a + \beta + b_0 \end{aligned} \tag{1}$$

Here, a denotes the annihilation operator for the cavity mode, defined in an appropriate rotating frame, (see Bachor and Ralph [2004]; Gardiner and Zoller [2000]). We have written $\kappa = \kappa_0 + \kappa_1 + \kappa_L$, where κ_0, κ_1 and κ_L quantify the strength of the couplings of the respective optical fields to the cavity.

It is clear that the cavity dynamics in (1) contain a nonlinear product term $\Delta\, a$, and we need to use a standard linearization method to obtain linear equations.

Let α denote the steady state average of a when $\Delta = 0$, so that $0 = -\frac{\kappa}{2}\alpha - \sqrt{\kappa_0}\beta$ and hence $\alpha = -\frac{2\sqrt{\kappa_0}}{\kappa}\beta$, which is a real number. We write $a = \alpha + \tilde{a}$, so that the linearized operator $\tilde{a}$ satisfies (neglecting higher order terms)

$$\dot{\tilde{a}} = -\frac{\kappa}{2}\tilde{a} - i\Delta\alpha - \sqrt{\kappa_0}b_0 - \sqrt{\kappa_1}b_1 - \sqrt{\kappa_L}b_L. \tag{2}$$

The linearized output field operator $\tilde{b}_{out}$ is given by

$$\tilde{b}_{out} = \sqrt{\kappa}_0 \tilde{a} + b_0 \tag{3}$$

since $b_{out} = \sqrt{\kappa}_0 \alpha + \beta + \tilde{b}_{out}$.

3.2 Quadrature Measurement

We model the measurement of the X_ϕ quadrature of $\tilde{b}_{out}$ with homodyne detection by changing the coupling operator for the laser mode to $\sqrt{\kappa}_0 e^{-i\phi} a$, and measuring the real quadrature of the resulting field. The linearized equations (2) and (3) become

$$\dot{\tilde{a}} = -\frac{\kappa}{2}\tilde{a} - i\Delta\alpha - \sqrt{\kappa}_0 e^{-i\phi} b_0 - \sqrt{\kappa}_1 b_1 - \sqrt{\kappa}_L b_L \tag{4}$$

and $\tilde{b}_{out} = \sqrt{\kappa}_0 e^{-i\phi}\tilde{a} + b_0$. Note that here, $b_0(t)e^{-i\phi}$ has been relabeled $b_0(t)$. The measurement signal is

$$\tilde{y} = \tilde{b}_{out} + \tilde{b}_{out}^\dagger = \sqrt{\kappa}_0 (e^{-i\phi}\tilde{a} + e^{i\phi}\tilde{a}^\dagger) + q_0 \tag{5}$$

where $q_0 = b_0 + b_0^\dagger$ is a standard Gaussian white noise.

We are now ready to express the cavity dynamics in state-space form. To this end, we re-express the cavity dynamics as follows. We will write $\tilde{q} = \tilde{a} + \tilde{a}^\dagger$, $\tilde{p} = \frac{\tilde{a} - \tilde{a}^\dagger}{i}$ for the cavity quadratures. Then in matrix form equations (4) and (5) for the linearized cavity model and sensor output become

$$\begin{aligned}
\begin{bmatrix} \dot{\tilde{q}} \\ \dot{\tilde{p}} \end{bmatrix} &= \begin{bmatrix} -\frac{\kappa}{2} & 0 \\ 0 & -\frac{\kappa}{2} \end{bmatrix} \begin{bmatrix} \tilde{q} \\ \tilde{p} \end{bmatrix} + \begin{bmatrix} 0 \\ 2\alpha \end{bmatrix} \Delta \\
&\quad - \sqrt{\kappa}_0 \begin{bmatrix} \cos\phi & -\sin\phi \\ \sin\phi & \cos\phi \end{bmatrix} \begin{bmatrix} q_0 \\ p_0 \end{bmatrix} \\
&\quad - \sqrt{\kappa}_1 \begin{bmatrix} 1 & 0 \\ 0 & 1 \end{bmatrix} \begin{bmatrix} q_1 \\ p_1 \end{bmatrix} \\
&\quad - \sqrt{\kappa}_L \begin{bmatrix} 1 & 0 \\ 0 & 1 \end{bmatrix} \begin{bmatrix} q_L \\ p_L \end{bmatrix}; \\
y &= k_2 \sqrt{\kappa}_0 \begin{bmatrix} \cos\phi & \sin\phi \end{bmatrix} \begin{bmatrix} \tilde{q} \\ \tilde{p} \end{bmatrix} \\
&\quad + k_2 \begin{bmatrix} 1 & 0 \end{bmatrix} \begin{bmatrix} q_0 \\ p_0 \end{bmatrix} + w_2
\end{aligned} \tag{6}$$

with noise quadratures $q_j = b_j + b_j^\dagger$, $p_j = \frac{q_j - p_j^\dagger}{i}$, for $j = 0, 1, L$ (all standard Gaussian white noises). Here, y is the sensor output in which we have included a sensor noise term w_2. Also, k_2 is a gain parameter defining the sensitivity of the sensor; see Huntington et al. [2007].

3.3 Identification of the Cavity Transfer Function

The cavity system, which comprises of both the electromechanical subsystem and the optical cavity is identified under closed-loop conditions.

In particular, although the optical subsystem can be modelled physically as in Sec. 3.2, the parameters in this model cannot be easily determined experimentally. Also, the electromechanical subsystem exhibits highly complex dynamics and is not easy to model physically. Hence, we are forced to obtain our complete model via system identification. A proportional-integral (PI) controller (whose coefficients are adjusted by trial and error) is used to stabilize the system to allow measurement of the system under closed-loop conditions. The gain and the phase of the plant is directly determined for each frequency point within a suitable frequency range using a digital signal analyzer (DSA) (HP 35665A). The system is configured as shown in Fig. 4. The plant is excited with a sinusoidal input from the DSA and the outputs, control signal u and measurement signal y, are fed back to the DSA inputs. This setup allows us to directly measure the transfer function of the plant.

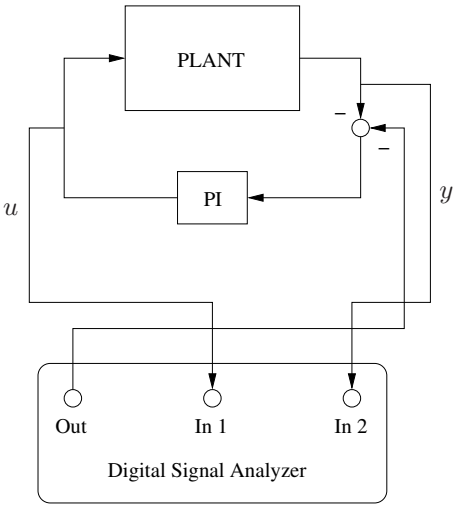

Fig. 4. System setup used for direct determination of plant transfer function in closed-loop condition.

The frequency response data obtained is fitted to an 8^{th} order model using a subspace identification method, McKelvey et al. [1996]. The algorithm we use accommodates arbitrary frequency spacing, and is guaranteed to exactly estimate any finite-dimensional transfer function, given a finite number of data (depending on the model order). The algorithm is also known to have provided good results with flexible structures, making it suitable for our application which includes a piezo-electric actuator coupled to the cavity mirror. Fig. 5 shows the gain(dB) and the phase of the measured frequency data points and the Bode plot of the identified system.

The system identification approach leads to a model in state-space form as follows:

$$\begin{aligned}
\dot{x} &= Ax + Bu; \\
y &= Cx.
\end{aligned} \tag{7}$$

3.4 Model of the Optical Cavity

Using (6), the Bode plot of the transfer function for the optical cavity from Δ to y in Fig. 3 will be of the form shown in Fig. 6. In particular, for our cavity, the corner frequency $-\frac{\kappa}{2}$ in (6), will be in the order of 10^5 Hz, which is well beyond the frequency range of interest for the LQG integral controller design. Hence, in constructing our LQG cost functional, we can safely replace Δ by y.

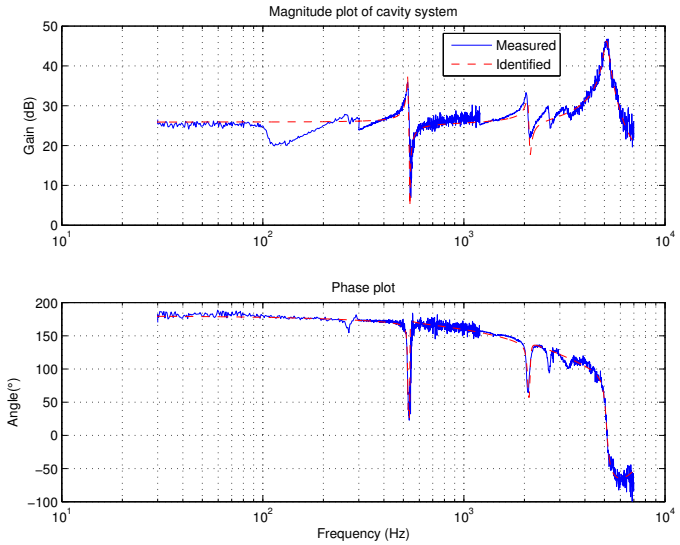

Fig. 5. Measured Frequency Response Data and Identified Model of the System.

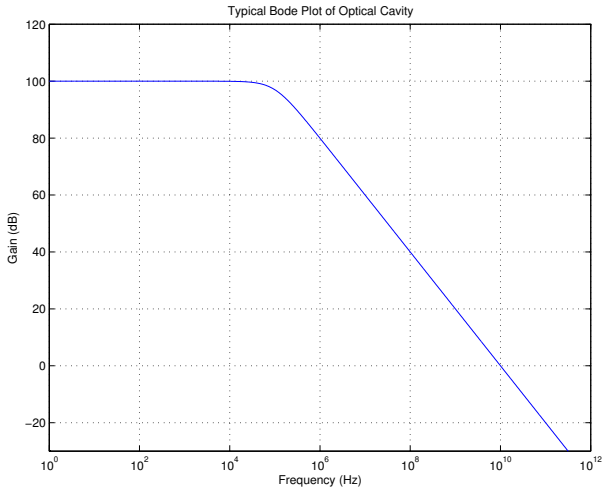

Fig. 6. Typical gain response for the optical subsystem

4. LQG INTEGRAL CONTROLLER DESIGN

4.1 LQG Performance Criterion and Integral Action

The LQG performance criterion to be used should encode the desired performance, namely to (i) keep the frequency error Δ small (ideally zero), and (ii) not use too much control energy. However, in our case, the system is also subject to frequency noise from the laser which drives the cavity. This laser frequency noise is most significant at low frequencies and presents itself as a slowly varying disturbance. An LQG performance criterion as described above will not provide satisfactory performance in the face of such a disturbance. This is the justification for including integral action in the LQG controller design. Integral action is included by adding an additional term in the cost function which involves the integral of the output. Furthermore, we also generate an additional fictitious output of the system by integrating the output y. This new output $\int y\,dt$ is also fed to the Kalman filter, which when combined with an optimal state feedback control law leads to an LQG integral optimal controller. This controller meets the desired performance requirement as described above as well as rejecting low frequency disturbances; e.g., see Grimble [1979]. Fig. 7 shows the setup used for the LQG integral controller design.

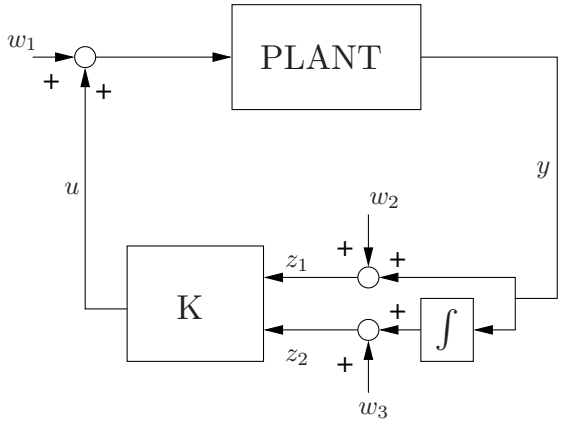

Fig. 7. Setup used for integral LQG controller design

From Fig. 7, the system can be described in state-space form as follows:

$$\begin{aligned}\dot{\tilde{x}} &= \tilde{A}\tilde{x} + \tilde{B}w_1 + \tilde{B}u;\\ \tilde{z} &= \tilde{C}\tilde{x} + \begin{bmatrix} w_2 \\ w_3 \end{bmatrix},\end{aligned} \tag{8}$$

where

$$\tilde{x} = \begin{bmatrix} x \\ \int y\,d\tau \end{bmatrix} \quad \text{and} \quad \tilde{z} = \begin{bmatrix} z_1 \\ z_2 \end{bmatrix}$$

and the matrices $\tilde{A}, \tilde{B}, \tilde{C}$ are constructed from the matrices A, B, C in (7) as follows:

$$\tilde{A} = \begin{bmatrix} A & 0 \\ C & 0 \end{bmatrix}, \quad \tilde{B} = \begin{bmatrix} B \\ 0 \end{bmatrix}, \text{ and } \tilde{C} = \begin{bmatrix} C & 0 \\ 0 & I \end{bmatrix}.$$

In equation (8), w_1 represents mechanical noise entering the system which is assumed to be Gaussian white noise with variance ϵ_1^2. Also, w_2 represents the sensor noise entering the system output y, which is assumed to be Gaussian white noise with variance ϵ_2^2. The quantity w_3 is included to represent sensor noise which enters the integrated output $\int y\,dt$. It is assumed to be Gaussian white noise with variance ϵ_3^2 and is included to fit into the standard framework of the LQG controller design. The parameters ϵ_1, ϵ_2 and ϵ_3 are treated as design parameters in the LQG controller design in Sec. 4.2.

The integral LQG performance criterion can be described as:

$$\mathcal{J} = \lim_{T\to\infty} \mathbf{E}\left[\frac{1}{T}\int_0^T [x^T Q x + u^T R u + L(y)^T \bar{Q} L(y)]dt\right] \tag{9}$$

where

$$L(y) = \int_0^t y(\tau)\,d\tau.$$

We choose the matrices Q, R and $\bar{Q}$ such that

$$x^T Q x = |y|^2, \quad u^T R u = r|u|^2, \text{ and } \bar{Q} = \bar{q},$$

where $r > 0$ and $\bar{q} > 0$ are also treated as design parameters.

The expectation in (9) is with respect to the Gaussian classical noise processes described previously, and the assumed Gaussian initial conditions. Given our system as described by (8), the optimal LQG controller is given by (e.g., see Kwakernaak and Sivan [1972])

$$u = -r^{-1}\tilde{B}^T X \hat{\tilde{x}}, \tag{10}$$

where

$$0 = X\tilde{A} + \tilde{A}^T X + \tilde{Q} - r^{-1} X\tilde{B}^T\tilde{B}X, \tag{11}$$

and

$$\tilde{Q} = \tilde{C}^T \begin{bmatrix} 1 & 0 \\ 0 & \bar{q} \end{bmatrix} \tilde{C}.$$

The observer dynamics are described by

$$d\hat{\tilde{x}} = \tilde{A}\hat{\tilde{x}}\,dt + \tilde{B}u\,dt + K[d\tilde{z} - \tilde{C}\hat{\tilde{x}}\,dt] \tag{12}$$

and for the case of uncorrelated process and measurement noises, the solution of the optimal observer is obtained by choosing the gain matrix

$$K = P\tilde{C}^T V_2^{-1}, \tag{13}$$

where

$$0 = \tilde{A}P + P\tilde{A}^T + V_1 - P\tilde{C}^T V_2^{-1}\tilde{C}P. \tag{14}$$

Here

$$V_1 = \epsilon_1^2\tilde{B}\tilde{B}^T = \mathbf{E}[w_1 w_1^T] \quad \text{and} \quad V_2 = \begin{bmatrix} \epsilon_2^2 & 0 \\ 0 & \epsilon_3^2 \end{bmatrix}$$

define the covariance of the process and measurement noises respectively.

4.2 Design Parameters

In designing the LQG controller, the design parameters ϵ_1^2 (the mechanical noise variance), ϵ_2^2 (the sensor noise variance of y), ϵ_3^2 (the sensor noise variance of $\int y$), r (the control energy weighting in the LQG cost function) and $\bar{q}$ (the integral output weighting in the LQG cost function) were adjusted for good controller performance. The values used are given in Table 1:

Design parameter	Value
ϵ_1	4×10^{-2}
ϵ_2	20
ϵ_3	5×10^{-4}
r	1×10^{-3}
$\bar{q}$	1×10^{8}

Table 1. Design Parameter Values

These parameter values led to an LQG controller which is then discretized using a first-order hold at a sampling frequency of 10 kHz. The Bode plots of the continuous and the discrete controller are shown in Fig. 8. The discrete bode plot becomes distorted at frequencies above the Nyquist frequency (5 kHz).

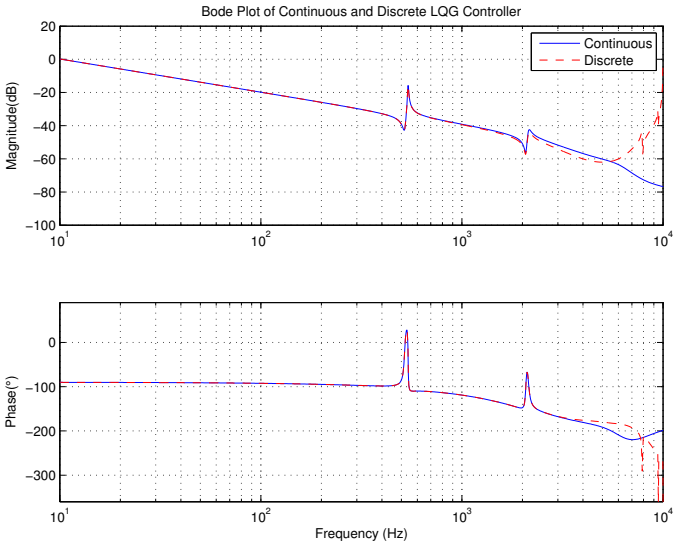

Fig. 8. Continuous and Discrete LQG controller Bode plot.

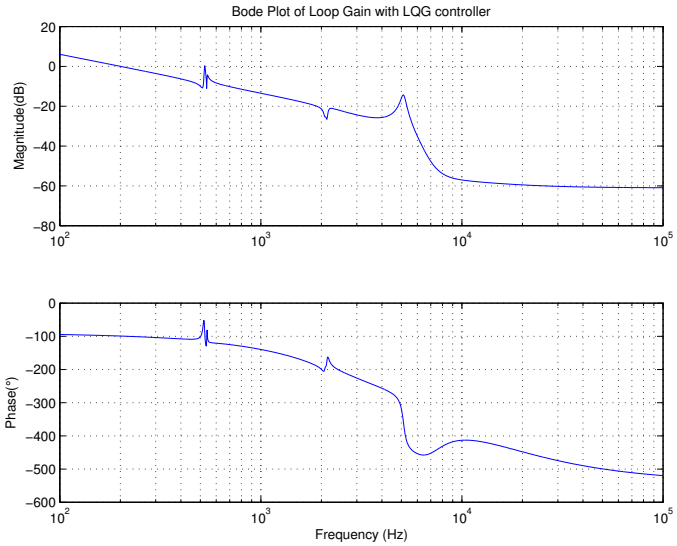

Fig. 9. Bode plot of Loop Gain L

Also, the corresponding loop gain Bode plot is shown in Fig. 9. The controller provides comfortable gain and phase margins of 19 dB and 78° respectively.

Finally, the gain of the closed-loop transfer function from control signal u to output y is shown in Fig. 10, which shows that the controlled system should have a bandwidth of about 200 Hz.

5. EXPERIMENTAL RESULTS

The discrete controller as described above is compiled to run on a dSpace DS1005 PPC Board at 933 MHz. The controller in place successfully stabilizes the frequency in the optical cavity, locking its frequency to that of the laser frequency, ω_0.

Fig. 11 shows a time history of the measurement gathered and control signal generated over a time period of 0.02 s. The measurement signal is the output of the homodyne detector y and is a reflection of the frequency error Δ. The

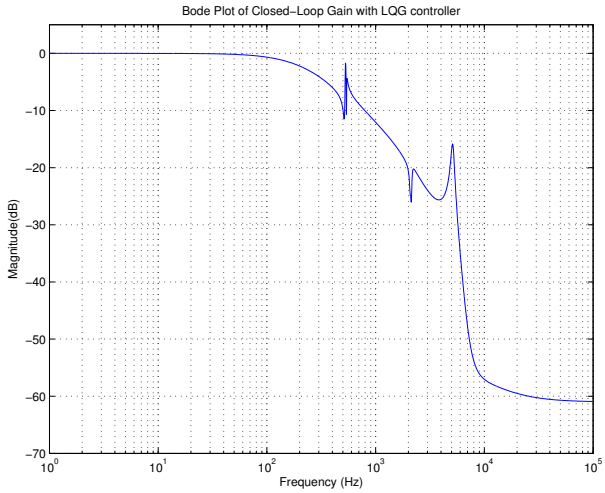

Fig. 10. Closed Loop Gain T from u to y

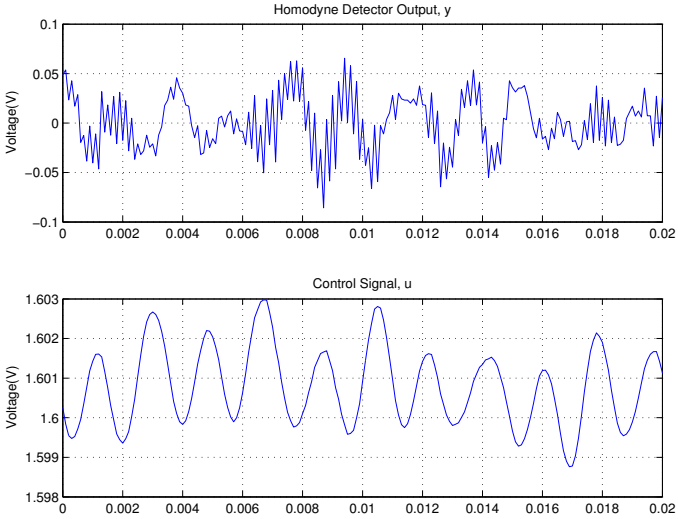

Fig. 11. Measurement and Control Signals

control signal generated is also as a consequence a signal of small magnitude that is superimposed over a d.c. offset voltage. This signal is amplified through a high-voltage (HV) amplifier in our system before being applied to the piezo-electric actuator, which in turn controls the position of the cavity mirror. It can be seen from Fig. 11 that even though we have achieved frequency stabilization, external disturbances from within the laboratory still excite to a small degree the resonances in the electromechanical system at frequencies of 500 Hz and 5 kHz approximately. Nevertheless, it can be safely stated that the experimental results obtained validate our modeling of the cavity system and confirm that the LQG integral controller design technique used is appropriate for this type of system.

6. CONCLUSION AND FUTURE WORK

In this paper, we have shown that a modern control technique such as LQG integral control can be applied to a problem in experimental quantum optics which has previously been addressed using classical control and an ad hoc technique measuring the normally unmeasurable quantity of the frequency error Δ. An important advantage of the LQG technique is that it can be extended in a straightforward way to multivariable control systems with multiple sensors and actuators. This will be investigated in future work in which we will consider the possibility of using additional actuators such as a phase modulator situated within the cavity or an additional piezo actuator to control the driving laser. The use of additional sensors will also be considered. Such sensors could include the use of a beam splitter and an additional homodyne detector to measure the other optical quadrature. Also, we may consider the use of accelerometers to provide additional measurements of the mechanical subsystem. Furthermore, we may wish to control the effects of air turbulence within the cavity and an additional interferometric sensor could be included to measure the optical path length adjacent to the cavity. Such a measurement would be correlated to the air turbulence effects within the cavity. The subspace approach to identification used to determine the plant is also particularly suited to multivariable systems. In addition, techniques for controller reduction will also be considered to reduce computational burden, especially as the model gets more complicated.

REFERENCES

H. A. Bachor and T. C. Ralph. *A guide to experiments in quantum optics*. John Wiley, 2004.

E. D. Black. An introduction to Pound-Drever-Hall laser frequency stabilization. *Am. J. Phys.*, 69(1):79–87, 2001.

S. C. Edwards and V. P. Belavkin. Optimal quantum feedback control via quantum dynamic programming. quant-ph/0506018, 2005.

C. W. Gardiner and P. Zoller. *Quantum noise*. Springer, Berlin, 2000.

M. J. Grimble. Design of optimal stochastic regulating systems including integral action. In *Proc. IEE*, volume 126, pages 841–848, 1979.

E. H. Huntington, M. R. James, and I. R. Petersen. Laser-cavity frequency locking using modern control. In *Proc. 46th IEEE Conf. Dec. & Cont.*, pages 6346–6351, New Orleans, Dec. 2007.

H. Kwakernaak and R. Sivan. *Linear optimal control systems*. Wiley, 1972.

T. McKelvey, H. Akçay, and L. Ljung. Subspace-based multivariable system identification from frequency response data. *IEEE Trans. Aut. Cont.*, 41(7):960–979, 1996.

A. J. Shaiju, I. R. Petersen, and M. R. James. Guaranteed cost LQG control of uncertain linear stochastic quantum systems. In *Proceedings of the 2007 Am. Cont. Conf.*, pages 2118–2123, New York, July 2007.